

MODEL BASED DEVELOPMENT OF EMERGENCY TRAJECTORIES FOR UNMANNED AERIAL VEHICLES

M. Kirchner and R. M. Leitner

IABG mbH, Innovation Centre, Einsteinstrasse 20, 85521 Ottobrunn Germany

Abstract

The model-based development of emergency descent trajectories is presented using the example of a helicopter as a function of flight limitation parameters. The trajectory ensures a fast coordinated and controlled emergency descent in the smallest possible space and from any flight condition. Although the model is based on a helicopter the trajectory can also be transferred to fixed-wing aircraft. The unmanned helicopter is on an aerial photography mission with constant trajectory speed and flight altitude. It should be possible to initiate the emergency descent at any time without exceeding the limiting parameters (e.g. roll time constant, build-up of vertical speed). To be able to perform a safe emergency descent in defined emergency descent areas, the space requirement must be determined in advance by e.g., a validated flight simulation. The seamless connection of the emergency descent in every attitude of the aerial photography flight, as well as the calculation of the trajectory, are the focus of the paper. The results are verified using desktop and real-time simulations with Pilot-on-the-Loop.

Keywords

UAV, Missionplanning, Flightmechanics

NOMENCLATURE

Formula symbols

M	Transformation matrix	-
\mathbf{n}	Vector of the load factors	gs
\mathbf{r}	Position vector	m
χ_K	Kinematic azimuth	rad
\ddot{h}	Kinematic climb acceleration	m/s ²
$\dot{\mu}_K$	Kinematic bank rate	rad/s
\dot{h}	Kinematic climb velocity	m/s
κ	Curvature	1/m
μ_K	Kinematic bank angle	rad
τ	Angle of the tangent	rad
c_i	Parameter of the sigmoid	-
g	Gravitational acceleration	m/s ²
h	Height above ground	m
l	Length	m
R	Radius	m
t	Time	s
V_K	Kinematic speed	m/s
x	Linear position along x-axis	m
y	Linear position along y-axis	m

1. MOTIVATION

Due to the progressive integration of small unmanned aerial vehicles (UAV) into the airspace, it is necessary to further increase safety in connection with manned aircraft. Especially with automated procedures, such as automatic waypoint flying, it is important to support the UAV pilot in emergency situations. Here, for example, environmental influences such as backlighting and size ratios that are difficult to assess (distance to other objects) prevent the UAV pilot from reacting quickly and correctly to dangerous situations. In addition to technologies for the detection and identification of airspace participants (e.g. FLARM, ADS-B), it is important to support the UAV pilot with flight guidance in exceptional situations. According to the new Drone regulations of the European Union, UAV pilots are obliged to perform evasive maneuvers in relation to manned air traffic participants. So, if a return to the home airfield or a manually controlled descent is not possible, the UAV pilot must still be brought safely and as quickly as possible out of the danger zone. The first step in this direction is the calculation of emergency descent trajectories as a function of flight limitation parameters, which ensure a fast coordinated, and controlled emergency descent in the smallest possible space and from the flight condition.

2. UAV AND NOMINAL TRACK

For model-based development of the emergency trajectories a helicopter UAV based on the Trex 450 platform developed by the manufacturer Align was used, see Figure 1.



FIG 1. CAD Model of the helicopter-based UAV

The electrically powered helicopter is equipped with a three-bladed rotor head to improve smoothness. The landing gear gives the helicopter a secure footing even in rough terrain through its four legs. Multibody dynamics and flight control of the helicopter-based UAV were implemented in Simulink[®] and executed on a real-time machine for testing purposes.

The nominal track, see Figure 2, that the helicopter flies in a not-emergency case corresponds to an aerial image trajectory as used for image flights, e.g. in land surveying.

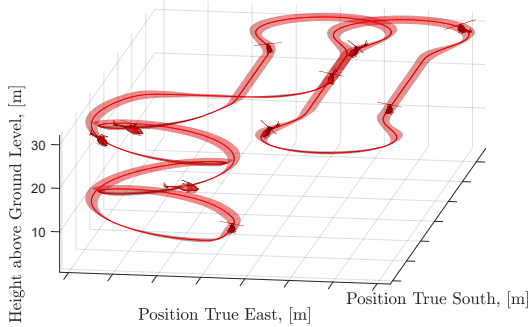


FIG 2. 3d representation of the nominal track

The UAV climbs to mission altitude h via a helix and winds with velocity V_K over the $a \times b$ terrain for image acquisition. At the end of the imaging flight, the UAV descends via an additional helix. Table 2 shows the design parameters of the nominal track, which includes kinematic constraints imposed by the UAV.

Description	Symbol	Value	Unit
Length	a	50	m
Width	b	50	m
Height above ground level	h	30	m
Kinematic speed	V_K	30km/h	
Max. kinematic bank angle	μ_{Kmax}	± 25	deg
Max. kinematic kinematic bank rate	$\dot{\mu}_{Kmax}$	± 20	deg/s
Max. kinematic climb-/sink velocity	\dot{h}_{max}	± 1.5	m/s
Max. kinematic climb-/sink acceleration	\dot{h}_{lim}	$\pm 0.3g_0$	m/s ²

TAB 1. Parameters and constraints of the nominal track

Detailed information about the helicopter-based UAV and the nominal track can be found in [1].

3. EMERGENCY DESCENT TRAJECTORY

Based on the track and the aircraft's allowable load factors, a fast and space-saving descent trajectory (i.e. to ensure the remote connection to the pilot) is generated. Therefore the altitude difference has to be defined. Also, the flight direction at the end of the descent shall be the same as at the descent point.

3.1. Space-saving geometry

To save as much space as possible the aircraft can not fly in a straight line. To be as close as possible to the descent point a circular trajectory is used. Therefore the radius of the circle $R_{K,min}$ is defined by the limiting load factor component $z n_{Bo,k}^{G,gg}$ and the kinematic velocity V_K regarding to following equation:

$$(1) \quad R_{K,min} = \frac{V_K^2}{\tan \left(\arccos \left(\frac{1}{z n_{Bo,k}^{G,gg}} \right) \right) g}$$

Since the kinematic bank rate, $\dot{\mu}_K$ is assumed to be constant, only a steady change of the bank angle μ_K and thus of the curvature κ is possible. To take this into account and to seamlessly connect the emergency descent trajectory at any slope angle of the track, a clothoid is applied. The length of the clothoid l_k is defined by the maximum kinematic bank rate $\dot{\mu}_{K,max}$, the limiting load factor component $z n_{Bo,k}^{G,gg}$ and the kinematic velocity V_K as follows:

$$(2) \quad l_k = \frac{\arccos \left(\frac{1}{z n_{Bo,k}^{G,gg}} \right) V_K}{\dot{\mu}_{K,max}}$$

The following parameter representation applies to a clothoid:

$$(3) \quad x_g(l_k) = \int_0^{L_k} \cos \frac{l_k}{2R} dl_k$$

$$(4) \quad y_g(l_k) = \int_0^{L_k} \sin \frac{l_k}{2R} dl_k$$

The figure below shows a clothoid transitioning from $\mu_K = 0$ to a circle of radius R_K . The clothoid has length l_k . The tangent angle $\tau = \frac{l_k}{2R}$ determines the angle of the segment of the circle crossed at the transition.

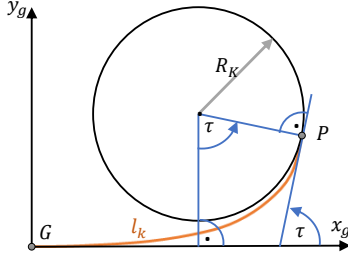


FIG 3. Clothoid transition

3.2. Fast altitude reduction

To achieve a fast descent, the maximum kinematic climb velocity \dot{h}_{max} must be reached without exceeding the limiting load factor component in vertical direction $_{max} \mathbf{n}_{Bo, \bar{k}}^{G, gg}$. The following formula describes the climb curve $h(t)$ with maximum kinematic climb acceleration \ddot{h}_{max} .

$$(5) \quad h(t) = h_0 - \frac{\ddot{h}_{max} t^2}{2}$$

The descent with definable altitude difference and length is not possible with the acceleration curve. This is not a problem for fast horizontal altitude descent. However, recovery in the same direction as the initiation is not possible.

3.3. End of maneuver

To fulfill both requirements (given height and inclined position at exit), the acceleration curve is not sufficient (too few degrees of freedom). The end of the trajectory is defined horizontally by the end of the circular path and the exit clothoid. Vertically, the height reduction to $h = h_{min}$ terminates the procedure. To bring both together, a transition element is needed. The following figures show the use of a sigmoid as a transition element. Since the clothoid is sometimes too short to completely close the vertical gap, a straight line is connected at the end of the clothoid.

A sigmoid is a real function that can be differentiated twice and has a positive derivative at every point. A sigmoid function also has exactly one inflection point W at half the run length where the slope is maximum. It approaches stationary end values with $x = \pm\infty$ and has the following function depending on:

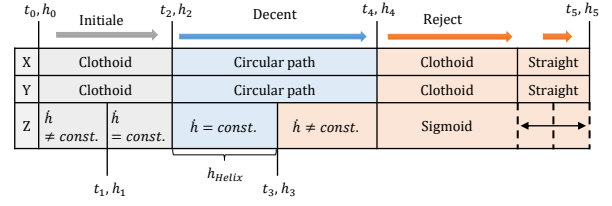


FIG 4. Progress of emergency descent with sigmoid

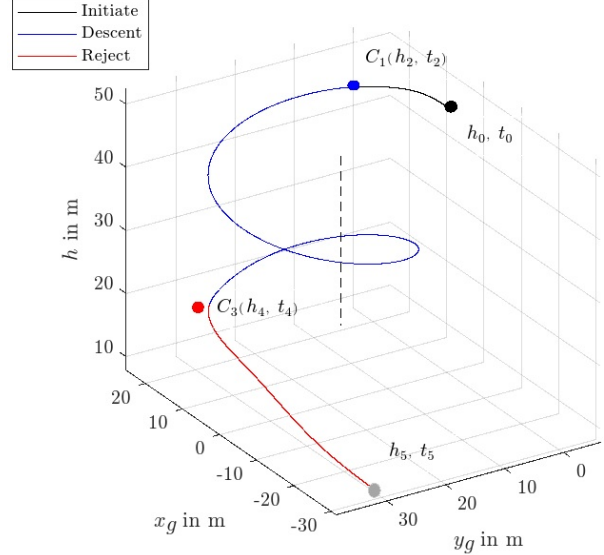


FIG 5. Emergency descent with sigmoid

$$(6) \quad y(x) = \frac{c_1}{1 + e^{-c_2 x}}$$

The parameter c_1 specifies the distance of the end values on the y-axis.

$$c_1 = |y(x_{+\infty}) - y(x_{-\infty})|$$

With c_2 the slope of the function can be defined.

Since the height difference $h_5 - h_4$ to be bridged is already fixed, the parameter $c_1 = h_5 - h_4$ is clearly defined. The parameter c_2 is iteratively calculated for $\ddot{h}_{max} \geq \ddot{h}$, thus approximating the kinematic climb acceleration \ddot{h} to the maximum kinematic climb acceleration \ddot{h}_{max} . For $c_2 \leq 0$ holds, where the extrema and thus the resulting kinematic climb acceleration increases with decreasing c_2 . Thus c_2 is decreased in infinitesimally small steps.

In the case of a very big gap or a very slow maximal kinematic climb acceleration or velocity, it could be better to not use a straight line because of saving space. For such a case it's better to use a waiting circular path. The descent ends at the predefined height and a circular path is added till the right azimuth χ_K is reached to fade out with the clothoid:

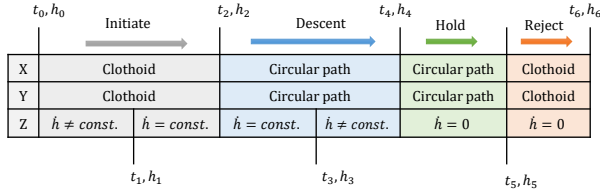


FIG 6. Progress of emergency descent with circular ending

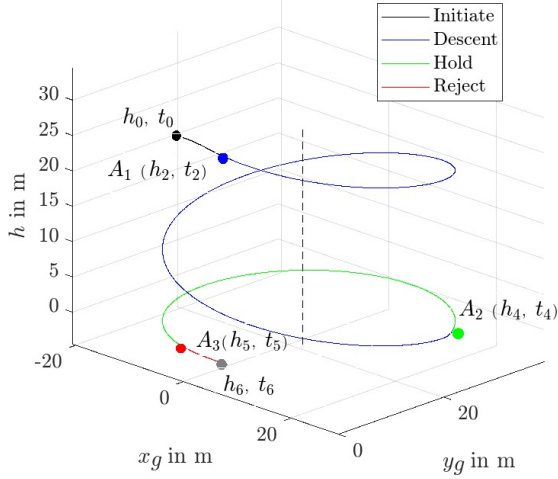


FIG 7. Emergency descent with circular path

4. IMPLEMENTATION

After discussing how the emergency trajectory works it needs to be implemented in a flying system with limited memory and processing capabilities. To save memory and computational power, the trajectory and the emergency trajectory are precomputed. To save memory, the trajectories are interpolated with the spline method. The following figure shows which calculations are performed before the flight (gray box) and which are performed during the flight in the aircraft (blue box):

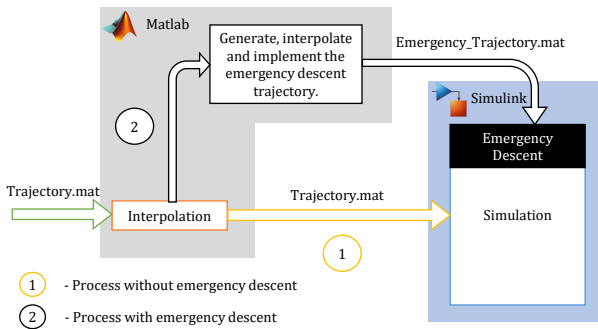


FIG 8. Generation process

As mentioned in the figure the inflight system gets two precomputed interpolated trajectories:

- 1) Normal flight trajectory
- 2) Emergency trajectory

In order to now be able to connect an emergency de-

scend at almost any point of the planned trajectory, it is necessary to extend the simulation model.

4.1. Function of the simulation model

The simulation model is of central importance because it determines the trajectory in the practical application on the aircraft or in real-time simulation. Thus, it provides the flight controller of the aircraft with the desired flight condition in real-time.

In the simulation, a runtime parameter traverses the flight path at the constant path velocity $V_K = const.$ This runtime parameter must now be redirected to the emergency descent trajectory by activating the emergency descent. Additionally, the emergency descent trajectory must be integrated into the existing trajectory in such a way that a seamless connection is established.

4.2. Adjustment of emergency descent trajectory

Since the descent helix has the minimum possible path radius (i.e., $\kappa_k = \kappa_{max}$), any curvature from $\kappa = 0$ to $\kappa = \kappa_{max}$ can be mapped on the initiation clothoid. For a seamless transition, the region where $\kappa < \kappa_k$ applied is cut (see Figure 17). However, this is only true for the x_g and y_g coordinates. The height profile of the z_g coordinate is continued identically. To bring both together, a straight line is inserted at the end of the path in the x-y plane

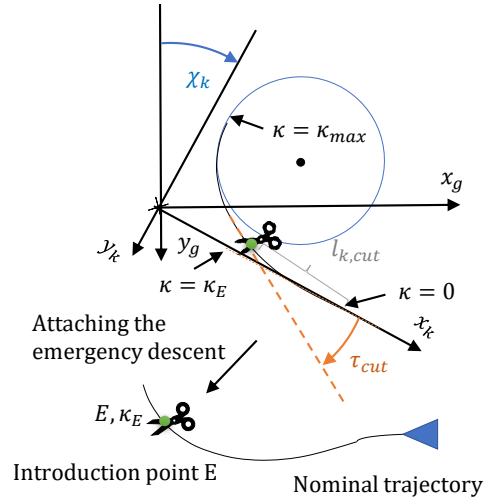


FIG 9. Connection of emergency trajectory

4.3. Redirection

To activate the emergency descent, the mission altitude ($\dot{h} = 0$) must be reached. Once activated, emergency descent cannot be deactivated again.

If emergency descent is initiated, the following values are extracted at the rejection point E :

- 1) curvature κ
- 2) sign of curvature (left- or right-curved)

3) kinematic azimuth χ_K

 4.4. Determining the clothoid run length to be cut $l_{k,cut}$ (Figure 17)

The curvature κ_E of the track at the rejection point E can be calculated using the following equation, cf. [2].

$$(7) \quad \kappa_E = \frac{\dot{x}_g \ddot{y}_g - \dot{y}_g \ddot{x}_g}{(\dot{x}_g^2 + \dot{y}_g^2)^{\frac{3}{2}}}$$

Since the initiation clothoid is cut off as described in chapter 4.2, the direction of rotation of the emergency descent is determined by the curvature. Since the interpolated trajectory has a curvature of $\kappa = 0$ only in rare cases, the decision is made independently of the available airspace. The sign of the curvature decides the direction of the descent spiral.

$$\kappa_E = \begin{cases} > 0 \rightarrow \text{left - turning} \\ \leq 0 \rightarrow \text{right - turning} \end{cases}$$

The runtime parameter $l_{k,cut}$ can be determined by applying the following equation, cf. [3].

$$(9) \quad l_{k,cut} = |\kappa_E| R_K l_k$$

This results in τ_{cut} for the tangent angle of the clothoid (Figure 17), after which the initiating clothoid must be cut:

$$(10) \quad \tau_{cut} = \frac{l_{k,cut} |\kappa_E|}{2}$$

4.5. Rotation of the descent helix

The descent spiral in the geocentric coordinate system must be transformed to the kinematic-coordinate system with angle $\chi_{K,E}$ and rotation matrix \mathbf{M}_{kg} .

$$(11) \quad \mathbf{r}_{EMG,k} = \mathbf{M}_{kg} \mathbf{r}_{EMG,g}$$

$$(12) \quad \mathbf{M}_{kg} = \begin{bmatrix} +\cos(\chi_K) & \sin(\chi_K) & 0 \\ -\sin(\chi_K) & \cos(\chi_K) & 0 \\ 0 & 0 & 1 \end{bmatrix}$$

For χ_K holds:

$$(13) \quad \chi_K = \tau_{cut} - \text{atan} \left(\frac{\dot{y}_g}{\dot{x}_g} \right)$$

Tests are required to verify the successful integration of the emergency descent. In the following, it is shown that both the trajectory and the docking process in Simulink and the real-time simulation with the flight controller meet the requirements.

5. VERIFICATION

To verify the results that the flight performance is not exceeded, tests must be performed in simulation and real-time simulation.

5.1. Verification with Simulink

To perform a verification check of the emergency descent trajectories, a velocity and acceleration profile can be created using Simulink. For this purpose, the derivatives are formed after the time t of the trajectory coordinates x_g , y_g and z_g . Since these derivatives are calculated numerically, the accuracy decreases with the height of the derivative.

In the following figures the course can be split into four parts:

- 1) Activation of the emergency descent
- 2) descent with constant velocity
- 3) Reduction of vertical speed
- 4) Filling the gap with a sigmoid function

 5.1.1. Kinematic climb velocity \dot{h}

In area 2 of the figure, it is clear that the limit of the vertical speed is minimally exceeded. After tests with other flight parameters, it can be determined that the deviation of $\leq 1\%$ results from the unavoidable rounding of a value in the program code. The overshooting at the transitions of the ranges 1, 2, and 3 and the resulting limit violations can be justified by the [4] phenomenon, which occurs during the spline interpolation [4].

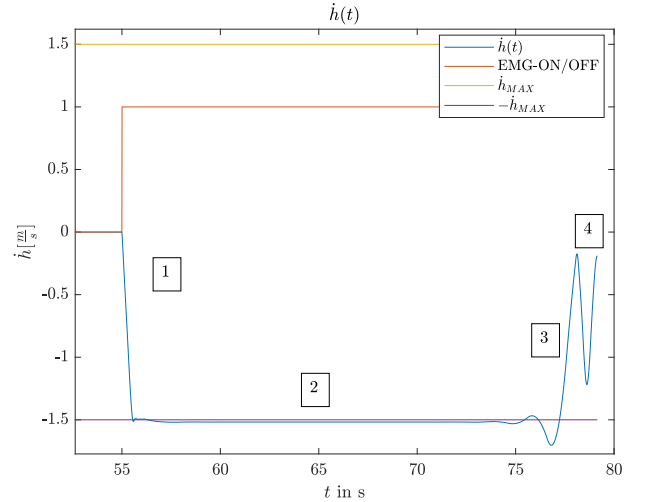


FIG 10. Progression of kinematic climb velocity $\dot{h}(t)$

 5.1.2. Kinematic climb acceleration \ddot{h}

Reading the kinematic climb acceleration \ddot{h} from the simulation proves unsuitable for checking the calculations due to the limited step size. As can be seen below in Sections 3 and 4, the Gibbs phenomenon gets worse, so a more detailed analysis is performed in the real-time simulation.

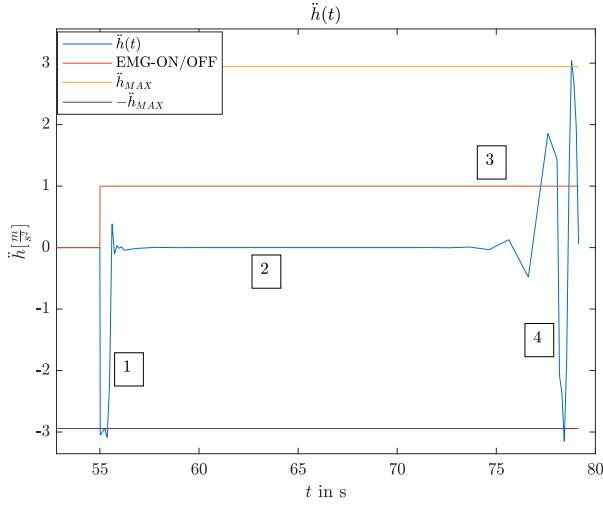


FIG 11. Progression of kinematic climb acceleration $\ddot{h}(t)$

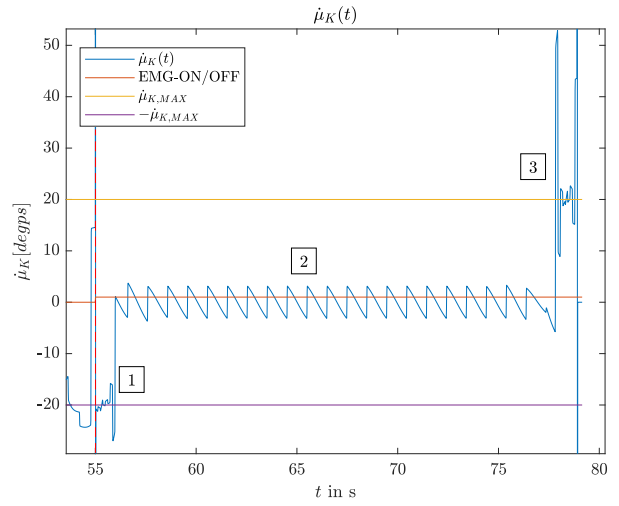


FIG 13. Progression of kinematic bank rate $\dot{\mu}_K(t)$

5.1.3. Kinematic bank angle μ_K

The kinematic bank angle μ_K depends on the curvature κ and is calculated numerically in the Simulink Simulation from the derivatives of the coordinates of the trajectory. In region 1 of the figure below, it can be seen that the kinematic bank angle is accompanied by a jump. This jump is caused by the lack of information about the initial value of the acceleration during the spline interpolation. It is necessary to consider this jump more precisely in the real-time simulation.

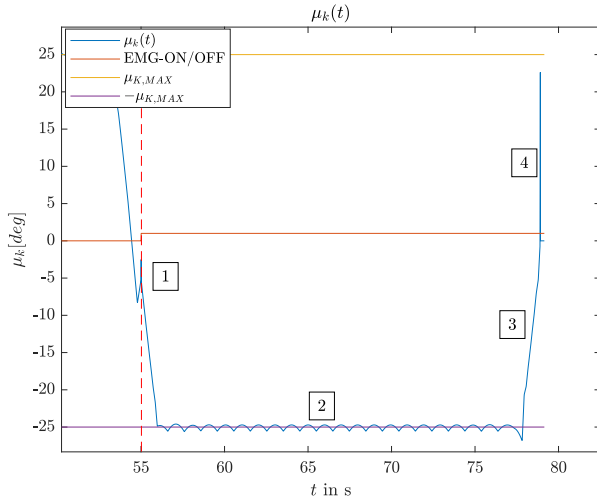


FIG 12. Progression of kinematic bank angle $\mu_K(t)$

5.1.4. Kinematic bank rate $\dot{\mu}_K$

In the kinematic bank rate plot (figures below), the effects of the Gibbs phenomenon are particularly evident. The limited step size means that an accurate analysis to meet the limits ($\pm\dot{\mu}_{K,max}$) cannot be performed.

5.2. Real-time simulation

As seen in the previous simulations using Simulink, there is a need for a better solution to prove the results. In this chapter, a real-time simulation with a real flight computer is used to obtain data. All data obtained from the simulation is not calculated by deriving values.

5.2.1. Kinematic climb velocity \dot{h}

As mentioned in the simulation part also in the real-time simulation, a slight overdrive in area 2 is visible in the kinematic climb velocity. In the area of the sigmoid (area 3, 4) everything looks normal and no limit is exceeded.

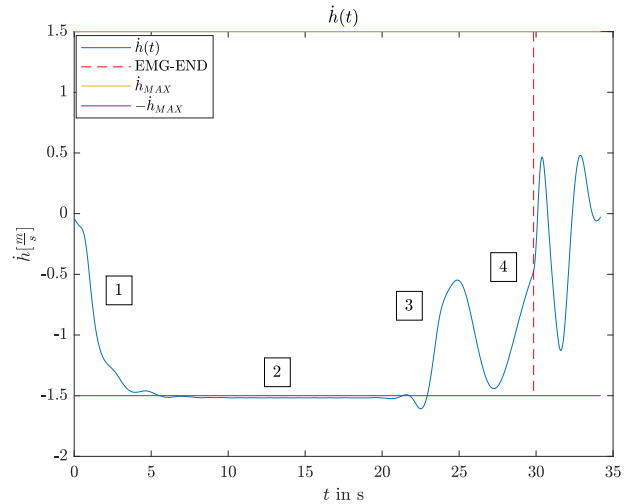


FIG 14. Progression of kinematic climb velocity $\dot{h}(t)$ in real-time simulation

5.2.2. Kinematic climb acceleration \ddot{h}

In the following figure of the kinematic climb acceleration, no overshoot can be seen as in the previous chapter. This is because the kinematic climb acceleration

cannot be built up abruptly in reality. In addition, the aircraft has a flight controller with feedback to control the altitude.

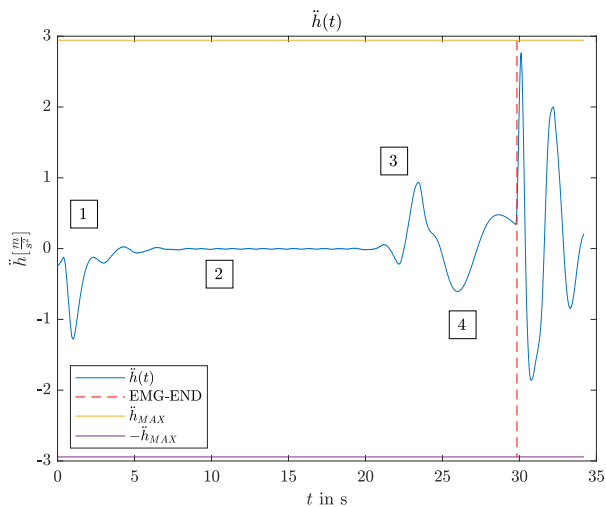


FIG 15. Progression of kinematic climb acceleration $\ddot{h}(t)$ in real-time simulation

5.2.3. Kinematic bank angle μ_K

The emergency descent divided into ranges 1-4 starts with the linkage of the emergency descent with the trajectory. In region 1, oscillatory deflection (Gibbs phenomenon) can be observed. Exceeding the maximum inclination angle of the trajectory (Figure 16 - yellow) is also due to the Gibbs phenomenon. In region 2 it is clear that the limit value of the trajectory inclination angle $\mu_{K,max}$ is not reached. The course of the kinematic bank angle μ_K goes towards zero in region 3, around which it oscillates in region 4.

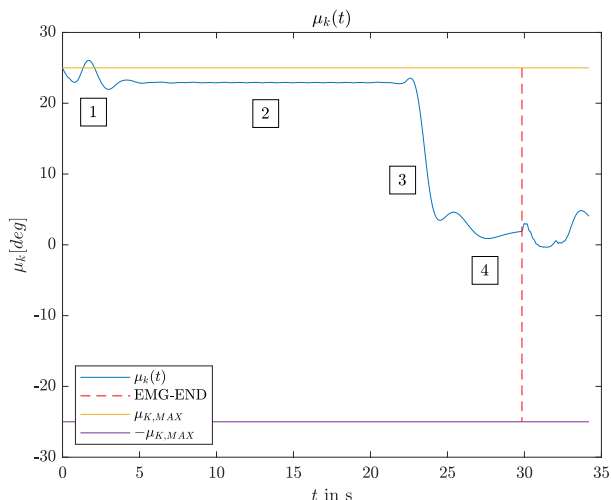


FIG 16. Progression of kinematic bank angle $\mu_K(t)$ in real-time simulation

5.2.4. Kinematic bank rate $\dot{\mu}_K$

In the beginning, a trajectory inclination angle is built up in region 1 in the lead-in clothoid. This can be seen

as a deflection in the course of the kinematic bank rate. In the course of the descent helix (area 2) the kinematic bank rate oscillates around zero due to the Gibbs phenomenon. In region 3 (rejection clothoid) the change of the kinematic bank angle leads to a deflection in the kinematic bank rate. In the area of the compensation line (area 4), the kinematic bank rate approaches zero. Likewise, no limit values are exceeded here.

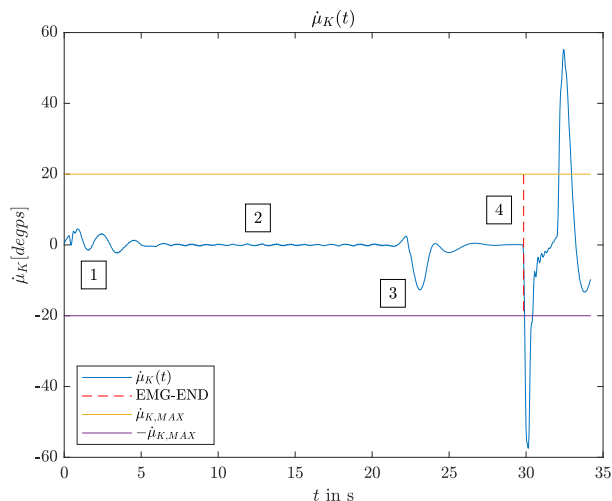


FIG 17. Progression of kinematic bank rate $\dot{\mu}_K(t)$ in real-time simulation

6. CONCLUSION AND OUTLOOK

The paper describes a complete system that allows emergency descents for rotorcraft and fixed-wing aircraft of any size. The trajectories were developed considering constraining flight parameters, provided that they automatically follow a predefined flight path with constant altitude. Looking to the future, it is particularly important to further develop and adapt the emergency descent system for use in different applications and scenarios. For example, it is possible to implement sensors that can detect obstacles and automatically initiate or abort emergency descents. The emergency descent system can also be extended to include an automatic landing function. Extending the system to also allow emergency descents on trajectories with variable altitude profiles would only be possible with real-time computation. Depending on the computing power on board the flight system, this may be realized in the future.

References

- [1] R. M. Leitner. Modelling and verification of helicopter multibody dynamics for different rotor configurations. PhD thesis, 2022.
- [2] Ilja N Bronstein, Juraj Hromkovic, Bernd Luderer, Hans-Rudolf Schwarz, Jochen Blath, Alexander Schied, Stephan Dempe, Gert Wanka, and Siegfried Gottwald. Taschenbuch der Mathematik, volume 1. Springer-Verlag, 2012.
- [3] Hugo Kasper, Walter Schürba, and Hans Lorenz. Die Klootoide als Trassierungselement. Dümmler, 1968.
- [4] FB Richards. A gibbs phenomenon for spline functions. *Journal of approximation theory*, 66(3):334–351, 1991.